FLUCTUATING PRESSURE ENVIRONMENTS AND HYDRODYNAMIC RADIAL FORCE MITIGATION FOR A TWO BLADE UNSHROUDED INDUCER

Andrew Mulder and Stephen Skelley
Fluid Dynamics Branch, Propulsion Division, Engineering Directorate,
NASA Marshall Space Flight Center
MSFC, AL

ABSTRACT

Fluctuating pressure data from water flow testing of an unshrouded two blade inducer revealed a cavitation induced oscillation with the potential to induce a radial load on the turbopump shaft in addition to other more traditionally analyzed radial loads. Subsequent water flow testing of the inducer with a rotating force measurement system confirmed that the cavitation induced oscillation did impart a radial load to the inducer. After quantifying the load in a baseline configuration, two inducer shroud treatments were selected and tested to reduce the cavitation induced load. The first treatment was to increase the tip clearance, and the second was to introduce a circumferential groove near the inducer leading edge. Increasing the clearance resulted in a small decrease in radial load along with some steady performance degradation. The groove greatly reduced the hydrodynamic load with little to no steady performance loss. The groove did however generate some new, relatively high frequency, spatially complex oscillations to the flow environment.

INTRODUCTION

During turbomachinery operation, the loads on the rotating shaft must be reacted by an arrangement of bearings. Regardless of the source of the load, such forces can cause excessive bearing wear and contact between the blade and the pump shroud, either of which can be detrimental to the safe, sustained operation of a liquid rocket engine turbopump. Hydrodynamically induced loads are usually considered to be insignificant compared to mechanical loads such as mass imbalance or eccentricity. However, water flow testing of a two blade unshrouded inducer exhibited a relatively large amplitude pressure oscillation with the potential for generating a problematic force. The oscillation is believed to be caused by a cavitation instability wherein the cavitation volume of one blade becomes larger than the one of the other blade. In the stationary reference frame this results in a pressure oscillation at shaft speed (1N). This is sometimes referred to as asymmetric cavitation. In the inducer reference frame, asymmetric cavitation is stationary, resulting in a static pressure imbalance that imparts a side load to the inducer shaft much like the force created by mass imbalance. This inducer underwent testing in the late summer of 2009 at the Marshall Space Flight Center (MSFC) Inducer Test Loop (ITL). During the winter of 2009 and spring of 2010, MSFC engineers checked out and installed a strain gage based rotating force measurement system in the ITL, and then used it to quantify the radial forces on the inducer shaft during operation. Water flow testing of two load mitigation configurations began in the late spring of 2010, and continued into the summer. In addition to the test campaign at MSFC, there was also test series using this inducer design at Concepts NREC at a different geometric scale and coupled to an impeller. Similar to the test at MSFC, objectives of this testing included the measurement of hydrodynamic radial loads and evaluation of a shroud configuration for load reduction. Testing at Concepts NREC occurred during the summer and fall of 2010.

Approved for public release; distribution is unlimited.

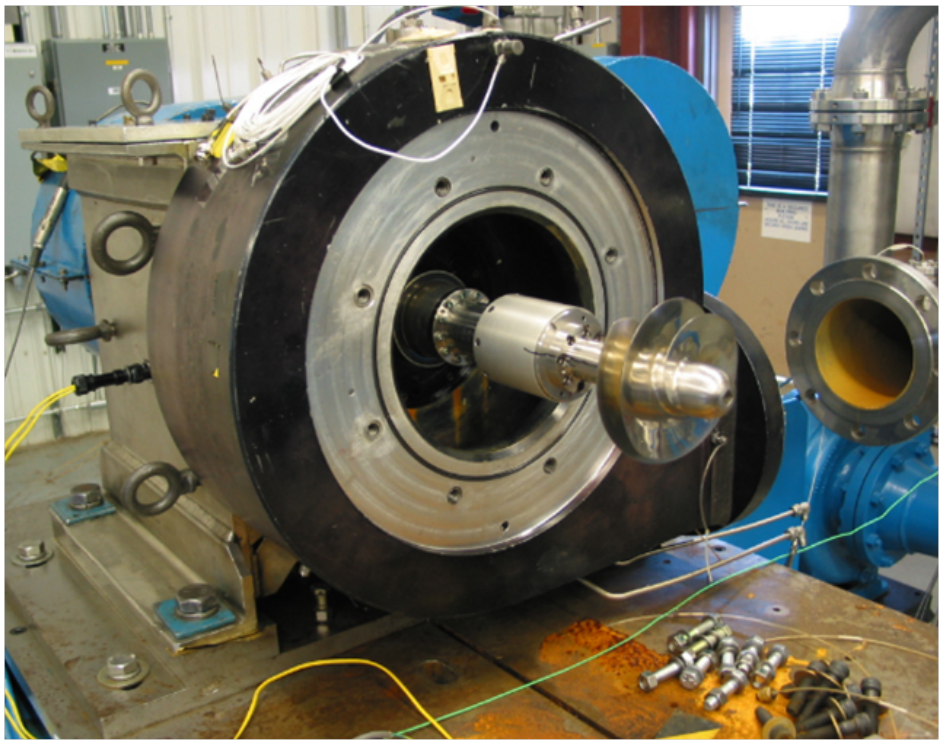

Figure 1: Rotating balance installed on the ITL, with inducer attached

TEST SETUP

The MSFC Inducer Test Loop is a closed water flow loop containing the test article inducer, a boost pump for fine flow control, a tortuous path valve for gross flow control, and a reservoir tank. Furthermore, it contains a de-aeration and particle filtration loop for maintaining water quality. The inducer diameter D for these water flow test series is 5.075 inches. The axial length L of the inducer is 1.42 inches.

The force measurement device, referred to as a rotating balance, is a six channel (three forces, three moments) strain gage device which can be installed as part of the drive shaft assembly. The inducer is mounted onto the balance itself; the rotating balance then senses all forces on the inducer shaft. See Figure 1 for a picture of the shaft/balance/inducer configuration. The balance has a measurement range of ± 100 lbf in the radial (normal and side) directions, and ± 1000 lbf in the axial direction. Specifically, the balance measurements are referenced to a particular location on the balance called the moment reference center. Figure 2 shows a schematic of this location relative to the inducer tip leading edge.

A 20 ring, air-cooled slip ring (Michigan Scientific Model SR20M/E512/X/ER) provided power to the balance and transferred signal from the rotating reference frame to the data acquisition system. Attached to the slip ring assembly, on the rotating side, were six strain gage amplifiers (Michigan Scientific Model AMP-SG3-U2-5). The amplifiers provided a gain of 100 to the relatively low balance strain gage output signals (on the order of millivolts) prior to sending the signals through the slip ring. In addition to the slip ring and rotating amplifiers, the amplifier/strain gage power supply (Model PS-AC) was also purchased from Michigan Scientific Corporation for this test. The slip ring assembly was mounted on the end of the inducer shaft opposite the inducer. See Figure 3 for a photograph of the ITL rotating assembly, including the inducer, balance, rotating amplifiers, and slip ring.

Multiple fluctuating pressure transducers (Kistler model 211B) were employed for this testing. The transducers were flush mounted in the inducer tunnel. There were several measurement planes located at various axial locations upstream, downstream, and directly over the inducer blades. Depending on the

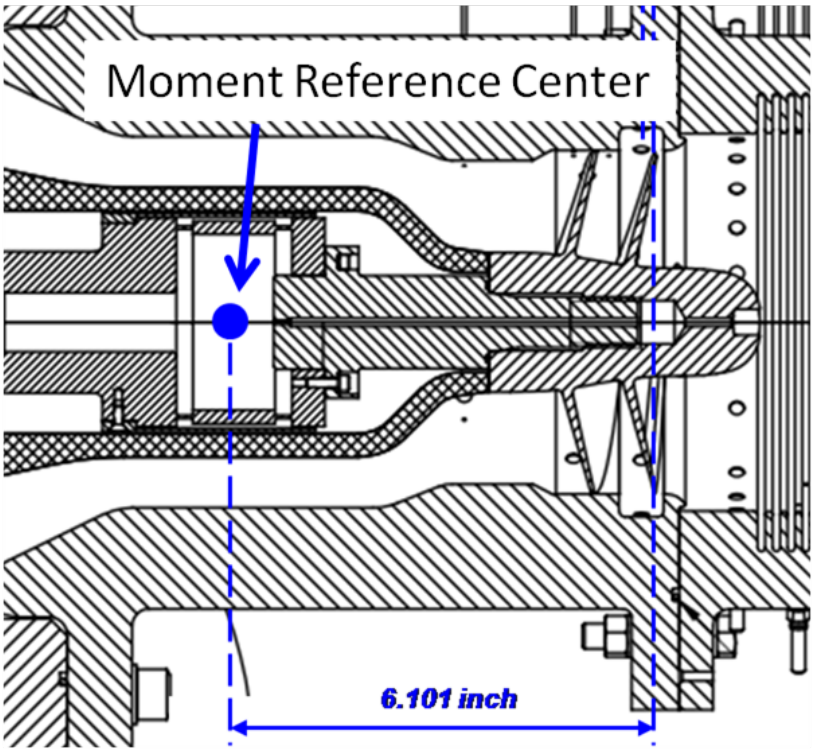

Figure 2: Test article schematic indicating the location of the balance moment reference center. The shroud shown here is from the grooved configuration.

measurement plane, there were as as many as seven transducers per plane and a few as one. These Kistlers are integral electronics piezoelectric (IEPE) devices, therefore the signals are AC coupled to the data recorder, that is, only the unsteady content of the pressure environment is captured with these transducers.

To compare fluctuating pressure data from one test configuration to another a single common measurement is used. This measurement is located 0.81 inches downstream of the inducer leading edge, which is slightly downstream of the groove location. Unless specifically stated, all fluctuating pressure quantities are from this reference measurement.

TEST PROCESS

During all test series, fluctuating pressure and force data were acquired while operating the inducer at constant shaft speed and flow rate, and while slowly and monotonically decreasing the reference inlet pressure from ambient down to inducer breakdown conditions. These pressure ramps were performed at flow rates ranging from 90% to 110% of the design flow coefficient, ϕ_D, in 5% increments.

DATA PROCESSING

It is useful to plot force and pressure results as a function of hydrodynamic operating conditions, i.e., flow coefficient and cavitation number. Flow coefficient (ϕ) is defined as the ratio of meridional flow velocity at the inducer inlet to the inducer blade tip speed, u_{tip}. Cavitation number (σ) is defined as the ratio of net positive suction pressure to tip dynamic pressure, $\frac{1}{2}\rho u_{tip}^2$.

Fluctuating pressure measurements were first analyzed in the time domain to check signal quality. If viable, the pressure signals were processed in a variety of ways to extract amplitude, frequency, and phase information. Analyses were made in the frequency domain using spectrograms, autospectra, frequency and amplitude trackings, and frequency/wave number spectra. Amplitude trackings for a specific

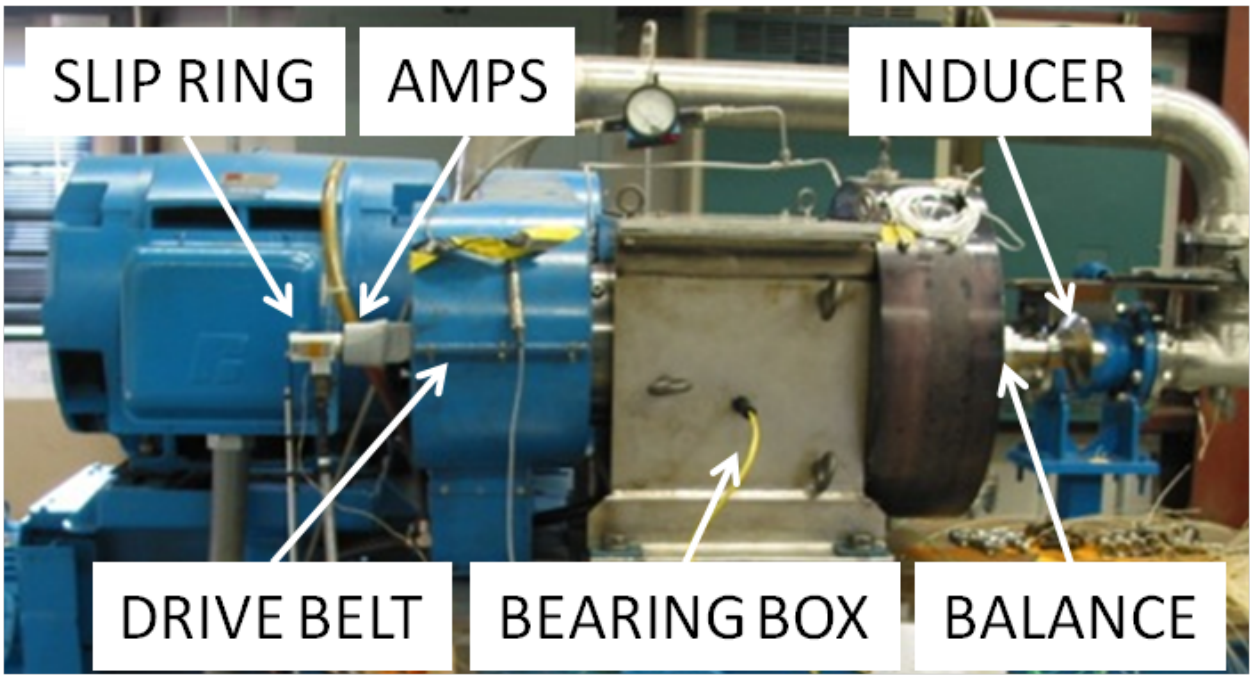

Figure 3: Photograph of the ITL rotating assembly

oscillation were processed such that the only energy present in the tracking bandwidth is due to the oscillation of interest. Fluctuating pressure amplitudes (p') are typically reported as RMS values, and are normalized by tip dynamic pressure, denoted with the symbol τ.

Raw rotating balance outputs were corrected for system electrical biases and then converted to engineering units in a process similar to that described in [1]. As mentioned previously, in the inducer reference frame asymmetric cavitation imparts a more or less stationary radial load to the inducer shaft. This means that the rotating balance data of interest is in the very low frequency range. After the conversion to engineering units, this stationary force was extracted by calculating the mean value of the force measurements. This was done by reducing the raw time histories with mean values over an appropriate time interval. The raw data are reduced in such a way that the mean value represents the low frequency content (0-2.5 Hz) of the data over 0.4 seconds. Mechanically induced radial loads are also present in this low frequency range; therefore, the resulting reduced data was a combination of hydrodynamic and mechanical forces. To isolate the hydrodynamic load, the mechanical load was quantified with an air spin test. The loads from the air spin test were processed in the same way as the water flow data, and because the only appreciable radial load in air should be due to mechanical sources, the air spin radial loads were used to subtract the mechanical load from the water flow data. The hydrodynamic radial force F is the root sum square of two appropriately reduced and orthogonal force measurements NF and SF. Based on the manufacturer's load calibration report [2] and a simple checkout test performed at MSFC, the accuracy of the final radial force calculation for all test series is within ± 0.7 lbf. Force results are reported in normalized form, where normalized force is defined as the ratio of the calculated force to the product of tip dynamic pressure and the cylindrical area swept by the inducer blade tip.

BASELINE TEST

Baseline water flow testing entailed an inducer with a blade tip clearance of 0.015 inches. Pressure ramps revealed a relatively clean fluctuating pressure environment. The most noticeable exception was an elevated synchronous (1N) pressure oscillation which was well defined within a particular range of cavitation numbers over the flow conditions as shown in Figure 4. These data come from a measurement plane 0.81 inches downstream of the inducer leading edge. Maximum fluctuating pressure values for the

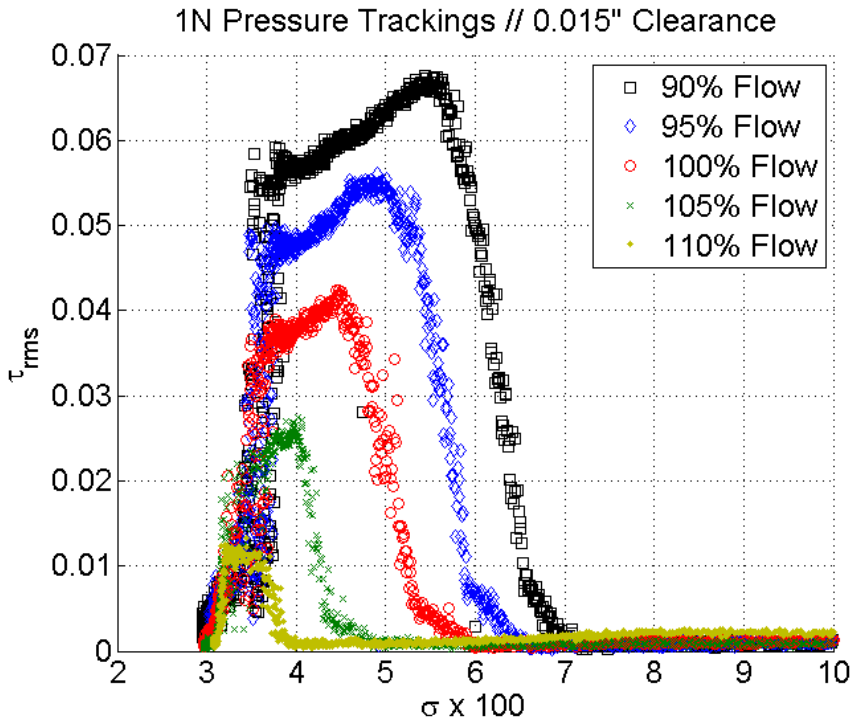

Figure 4: Synchronous amplitude trackings 0.81 inches downstream of the leading edge

1N oscillation at this location occur at $0.9\phi_D$ and a cavitation number of approximately 0.055, exceeding 6% of the tip dynamic pressure. For reference, during the period of elevated 1N oscillation, the wideband (10 Hz to 10 kHz composite) unsteady pressure spectral content at the same location over these same conditions approaches 10% of the tip dynamic pressure. Figure 5 is a plot of the maximum 1N amplitude at each of the measurement planes over the inducer blades. Based on the available measurements, the axial distribution of this oscillation shows that the center of maximum pressure is closer to the inducer leading edge than the trailing edge, at a peak value over 7% of the tip dynamic pressure. This indicates that the load caused by this oscillation would act somewhere in the upstream half of the inducer.

Figure 6 shows the hydrodynamic force for the baseline inducer tunnel. Comparing Figures 4 and 6, the elevated hydrodynamic force appears to be coincident with the elevated 1N pressure oscillation. Furthermore, since the rotating balance measures moments as well as forces, the moment arm of the hydrodynamic force can be estimated. Figure 7 is a plot of the moment arm relative to the inducer leading edge versus cavitation number. It supports the pressure information in that the peak hydrodynamic radial force is acting closer to the leading edge than the trailing edge. It also shows that the center of pressure of the asymmetric cavitation changes with cavitation number, presumably due to growth of the cavitation volumes and resulting flow asymmetry as inlet pressure goes down.

LOAD MITIGATION TESTS

The first method tested to reduce the hydrodynamic radial load was to uniformly increase the radial clearance over the inducer shroud from 0.015 inches to 0.028 inches. A larger clearance allows for two positive changes regarding hydrodynamic loads. First, the larger clearance provides less resistance to reverse flow at the inducer tip, therefore it changes the flow field and typically attenuates pressure oscillations in that region. Second, increasing the clearance means that the inducer can deflect farther without touching the shroud, making the maximum acceptable loading for rub margin larger. On the negative side, it should be noted that increasing the radial clearance typically has a deleterious effect on the steady inducer performance, namely the head rise and suction capability.

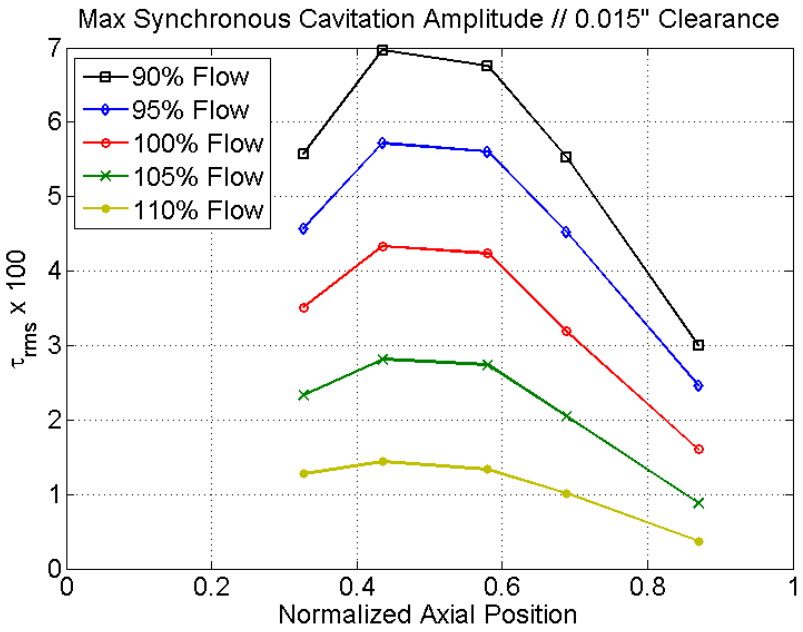

Figure 5: Axial distribution of the maximum 1N oscillation amplitude. On the abscissa, 0 denotes inducer leading edge and 1 denotes the trailing edge.

The second method tested to reduce the hydrodynamic load was to introduce a circumferential groove near the leading edge of the inducer. The concept of circumferential or axial grooves has been demonstrated to reduce or eliminate cavitation instabilities for other inducers by Shimiya *et al* [3] and Kang *et al* [4]. The groove acts locally as a very large radial clearance, which has a significant effect on the flow field in that region. The upstream edge of the groove was located 0.128 inches upstream of the inducer leading edge tip. The groove axial length was 0.661 inches, and the depth was approximately 0.336 inches. The radial clearance away from the groove was 0.014 inches. Because this relatively tight clearance is maintained over the downstream region of the inducer, the head rise is not debited as much as a uniform increase in radial clearance. Refer back to Figure 2 for a schematic of the groove configuration. An identical (except for geometric scale) groove design was used in the water flow testing at Concepts NREC.

LOAD MITIGATION RESULTS

The increased clearance test resulted in a fluctuating pressure environment much like that seen in the baseline test series, albeit at generally reduced amplitudes. The pressure environment was relatively clean, with a well defined region (in terms of σ and ϕ) of elevated synchronous fluctuating pressure with a corresponding hydrodynamic radial load. The grooved configuration resulted in a rather different fluctuating pressure environment, as will be discussed in a subsequent section, with relatively large reductions in synchronous fluctuating pressure and hydrodynamic radial force. Figure 8 is a plot comparing both the hydrodynamic radial force and the 1N fluctuating pressure results from the load mitigation tests to the baseline test. The plot is made using force values that are at least 80% of the magnitude of the peak measured force at each flow coefficient, along with the corresponding 1N pressure data. Besides showing the effects of the load mitigation configurations, a linear relationship between radial hydrodynamic force and synchronous fluctuating pressure is evident from this plot. Figure 9 directly displays the reduction in pressure and force values relative to the baseline test. This plot was made using the mean values from the data in Figure 8 at each flow coefficient. At the referenced measurement location 0.81 inches downstream of the inducer leading edge, increasing the clearance from 0.015 inches to 0.028 inches resulted in peak 1N oscillation amplitudes that were approximately 72% to 100% of the values measured in the baseline test, depending on flow coefficient. The hydrodynamic radial force values

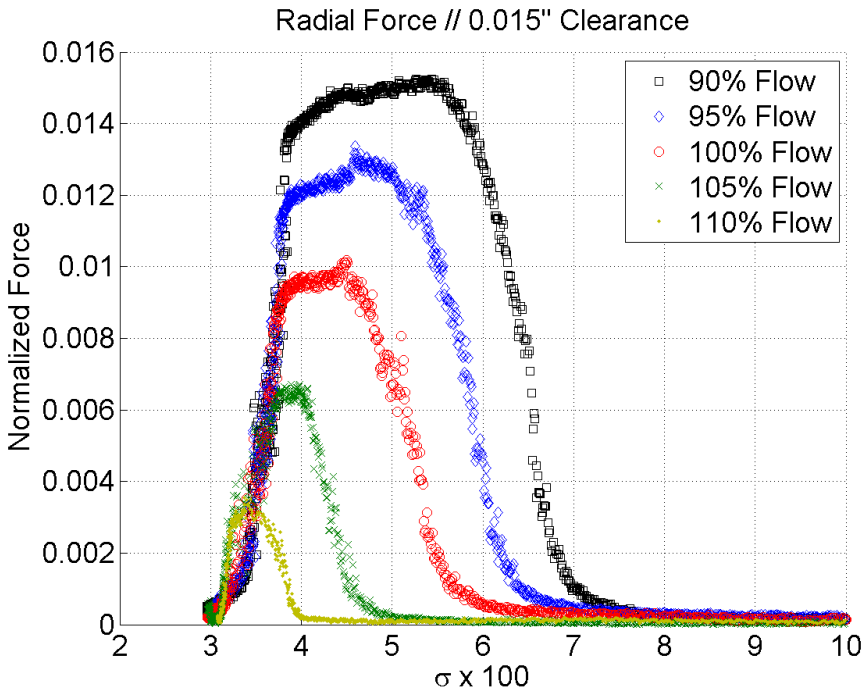

Figure 6: Inducer hydrodynamic radial load at various flow rates

were approximately 65% to 84% of the values measured in the baseline test. The groove configuration resulted in 1N pressure oscillations and hydrodynamic radial forces that were respectively 10% to 20% and 14% to 36% of the measured baseline values, depending on flow coefficient.

Load mitigation testing at Concepts NREC also utilized a circumferential groove, and achieved similar reductions in hydrodynamic load compared to a smooth tunnel.

Figure 10 is a plot comparing the inducer head coefficient Ψ across the three tested configurations at the design flow coefficient. Both the increased clearance test and grooved test head coefficients are lower than that seen in the baseline test at high cavitation numbers. When the cavitation number is in the range of the elevated synchronous pressure oscillation, the non-grooved tests experience a drop in head rise, while the grooved configuration head coefficient remains relatively constant. This figure also shows that the grooved configuration maintained the same suction performance as that seen in the baseline test. Unfortunately a comparison of suction performance for increased clearance test cannot be made with this plot, as that particular test did not reach breakdown conditions. Other test data suggest that the suction performance in the increased clearance test was probably only marginally worse than that observed in the baseline test.

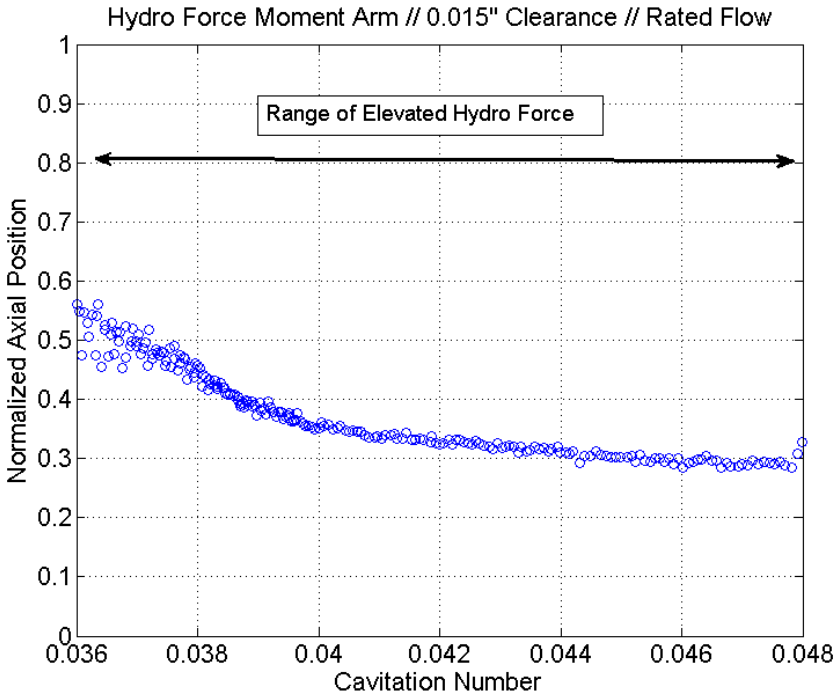

Figure 7: Axial location of the hydrodynamic radial force relative to the inducer. On the ordinate, 0 denotes inducer leading edge and 1 denotes the trailing edge.

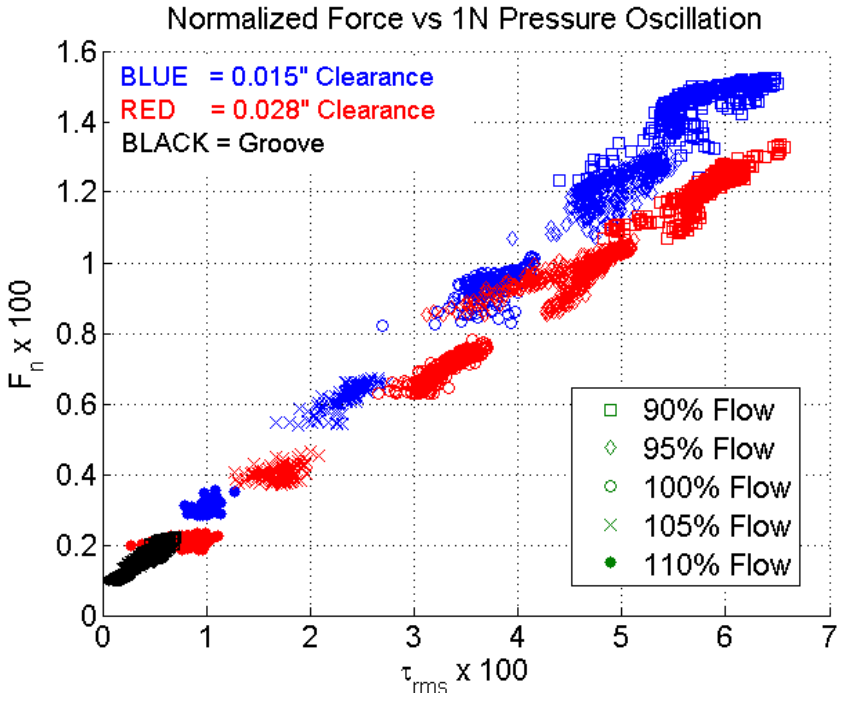

Figure 8: Peak normalized force plotted against peak normalized 1N pressure. Pressure data are from 0.81 inches downstream of the leading edge.

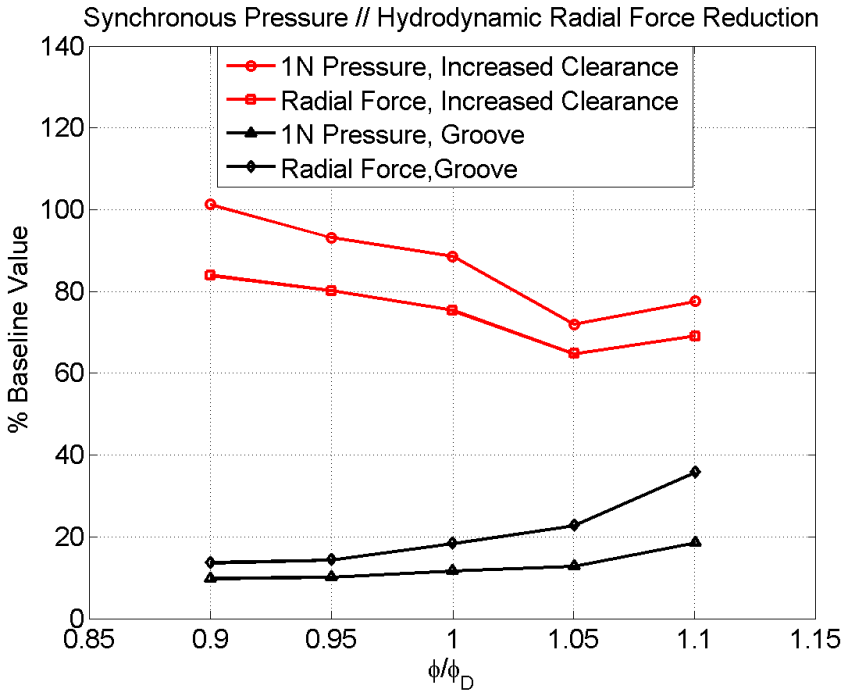

Figure 9: Pressure/Force reductions relative to the baseline test series plotted against flow coefficient

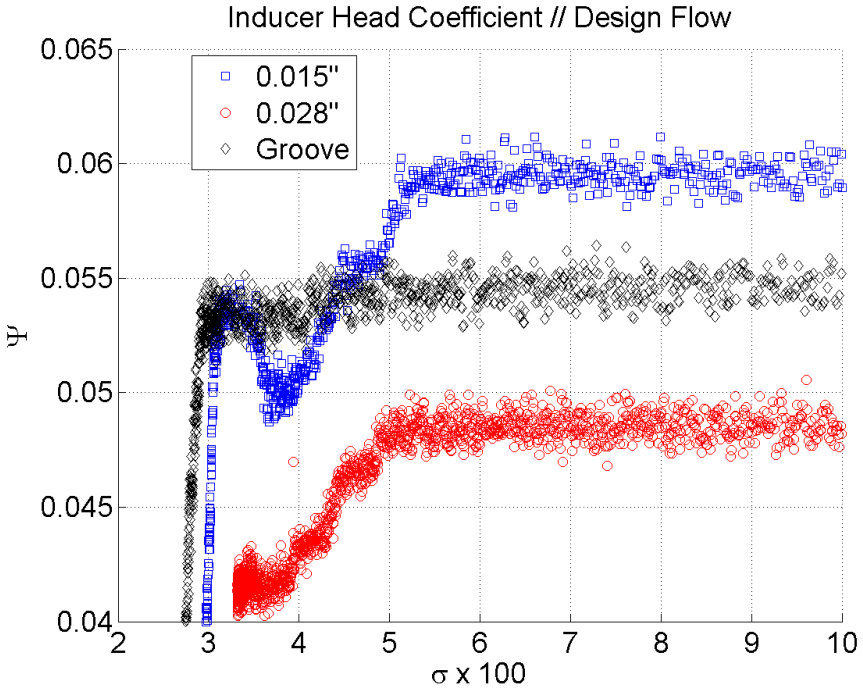

Figure 10: Head Coefficient comparison across all tested configurations at the design flow rate. The 0.028” test did not reach full breakdown conditions, unlike the other two tests.

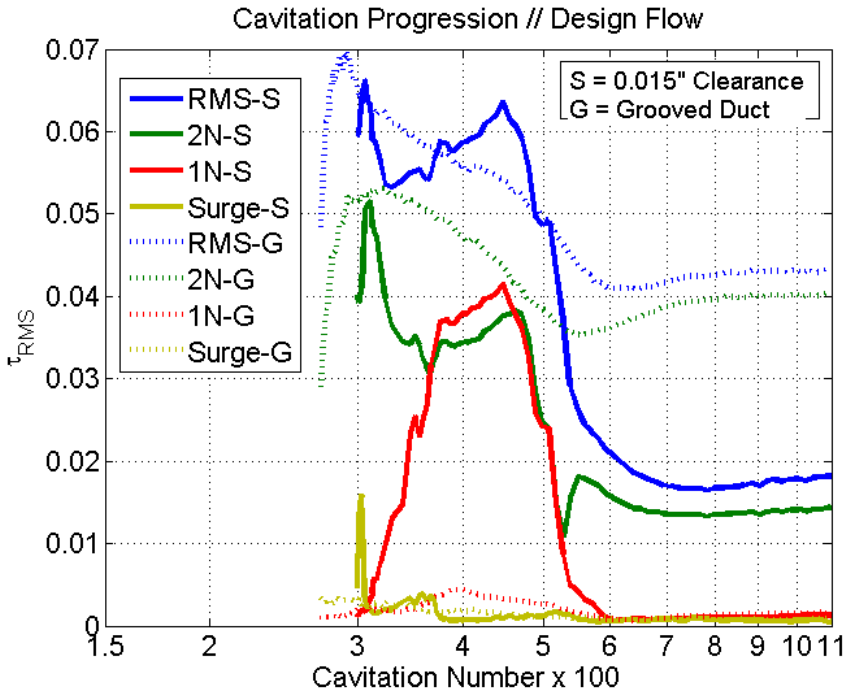

Figure 11: Comparison of various fluctuating pressure quantities between the baseline test and the grooved test. These trackings are from 0.81" downstream of the inducer tip leading edge.

GROOVE FLUCTUATING PRESSURE ENVIRONMENT

The fluctuating pressure environment generated by the groove configuration differed from the non-grooved configurations in more ways than just reducing the synchronous pressure oscillation and hydrodynamic radial force. In the non-grooved test series, a low frequency ($\sim$0.1N) surge oscillation occurred at cavitation numbers immediately below the conditions where the elevated 1N oscillations occurred. In the grooved configuration this oscillation was diminished in a similar fashion to the synchronous oscillation. Also, the blade passage oscillation (2N), which contains the bulk of the fluctuating pressure energy at high cavitation numbers, is elevated in the grooved test series when compared to the non-groove tests. Figure 11 contains plots of these comparisons at design flow conditions.

The groove also introduced a new set of oscillations to the unsteady environment over a wide range of operating conditions. Figure 12 shows the presence of multiple oscillations within the blade passages at non-integer values of shaft speed. Spatial analysis of these oscillations indicates that the pressure environment consists of multiple forward and backward spinning disturbances with as many as ten nodal diameters at some operating conditions, as shown in the frequency-wavenumber spectrum in Figure 13. Furthermore, the oscillations can be grouped according to the rotating reference frame frequency. Each oscillation measured in the laboratory frame is observed at a particular frequency in the rotating frame according to the relationship between the laboratory frame frequency and wave number:

$$f_{rotor} = f_{lab} + k f_N$$

Where f_{lab} is the frequency measured in the laboratory frame, f_N is the shaft speed, and k is the wave number where $k < 0$ denotes rotation in the same sense as the inducer shaft. For the oscillations detected in the groove testing, at any given operating conditions, most of the detectable oscillations map to a single frequency in the rotating frame. The frequencies of these oscillations are sensitive to both cavitation number and flow coefficient. In the range of 90% to 105% of the design flow condition, the on-rotor

frequencies were observed to reside within a frequency range of 9N-12N, depending on the specific hydrodynamic conditions. Figure 14 is a plot of autobicoherence for a measurement inside the groove. Bicoherence is high at almost all multiples of synchronous from 2N up to 16N. This indicates that the oscillation at the chosen reference frequency (0.69N) is modulating with all of those synchronous multiples to generate the oscillations observed in the laboratory reference frame. In other words, analysis of this fluctuating pressure data may indicate that the groove configuration generates a flow field instability that interacts or modulates with the inducer blade pressure wakes to create a relatively high frequency, spatially complex pressure environment around the inducer. This kind of environment would be of concern if any structrual elements near the inducer have natural frequencies in the same frequency range as the new oscillations. Also, because of some of the modulation products of this phenomenon have a wave number of zero (planar wave) these pressure disturbances could propagate away from the inducer.

Load mitigation testing with a circumferential groove at Concepts NREC also exhibited a similar phenonmenon, i.e. spatially complex oscillations, albeit with some differences in the exact frequencies and shapes that were observed at various operating conditions. Furthermore, spatially complex high frequency oscillations in the presence of a groove have been reported in the water flow tests by Kang *et al* [4].

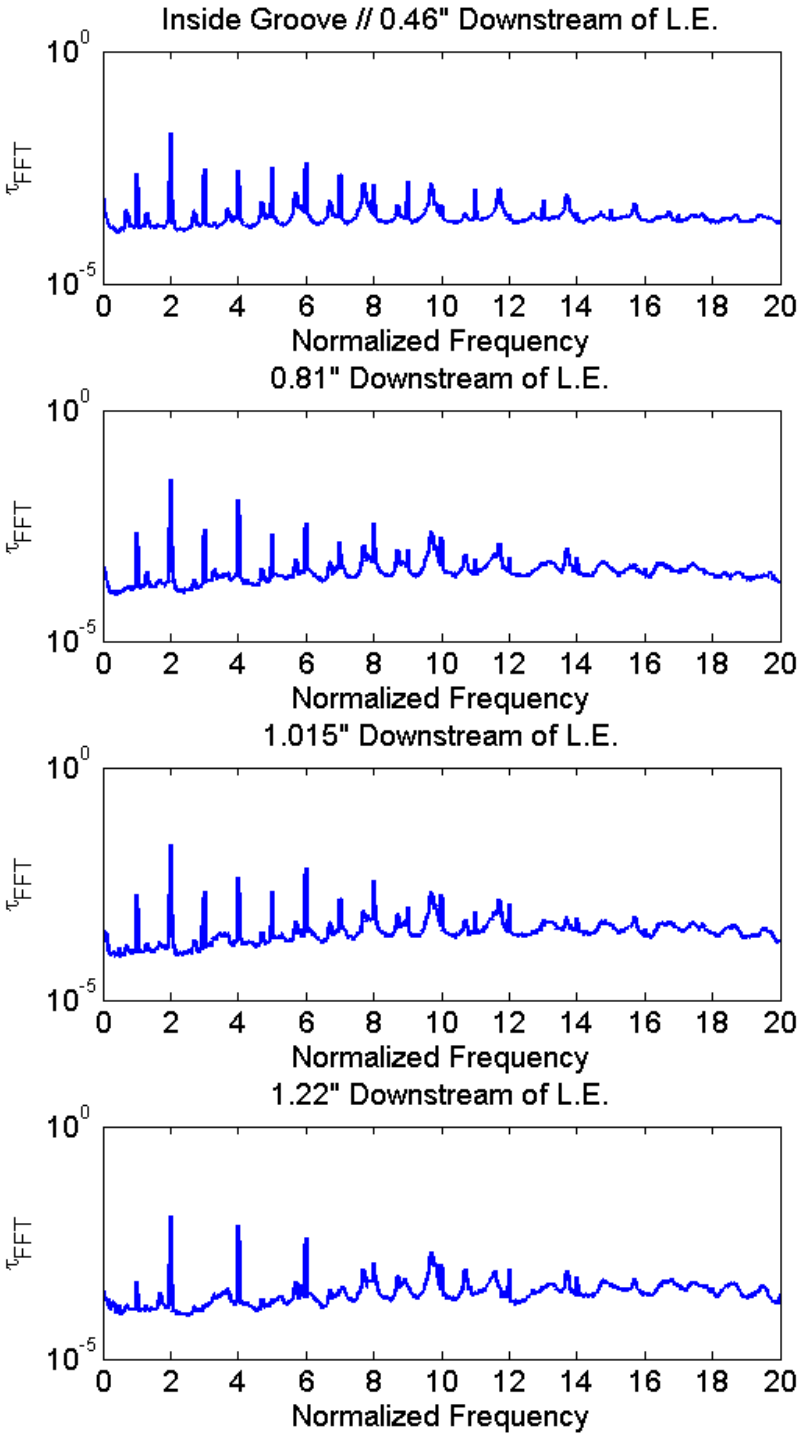

Figure 12: There are multiple oscillations at non-integer multiples of shaft speed in the blade passage measurement planes when the groove is present.

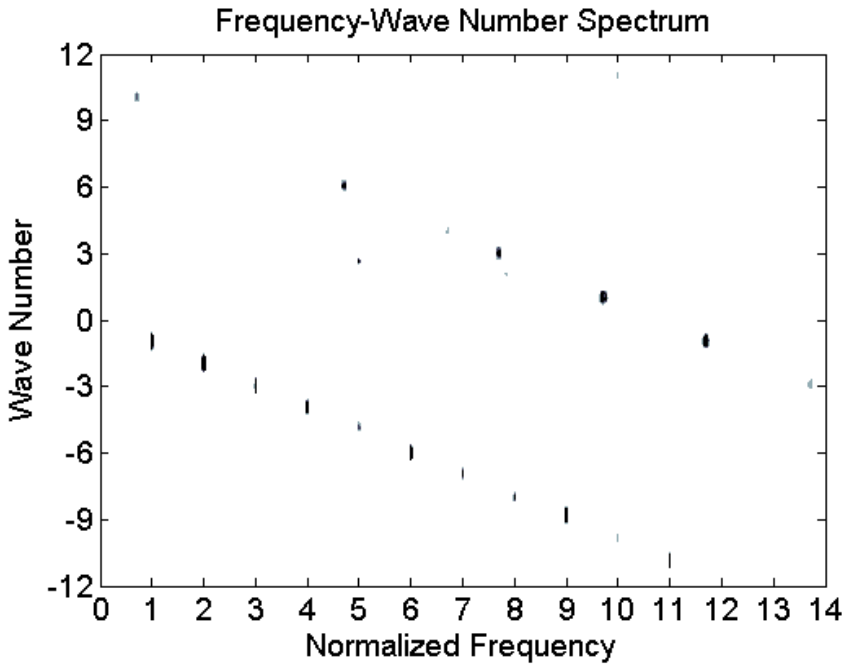

Figure 13: Frequency-Wave Number spectra from a measurement plane inside the groove at 92% rated flow. The lower diagonal shows the shapes generated by blade passage and harmonics. The upper diagonal is due to the groove induced oscillations.

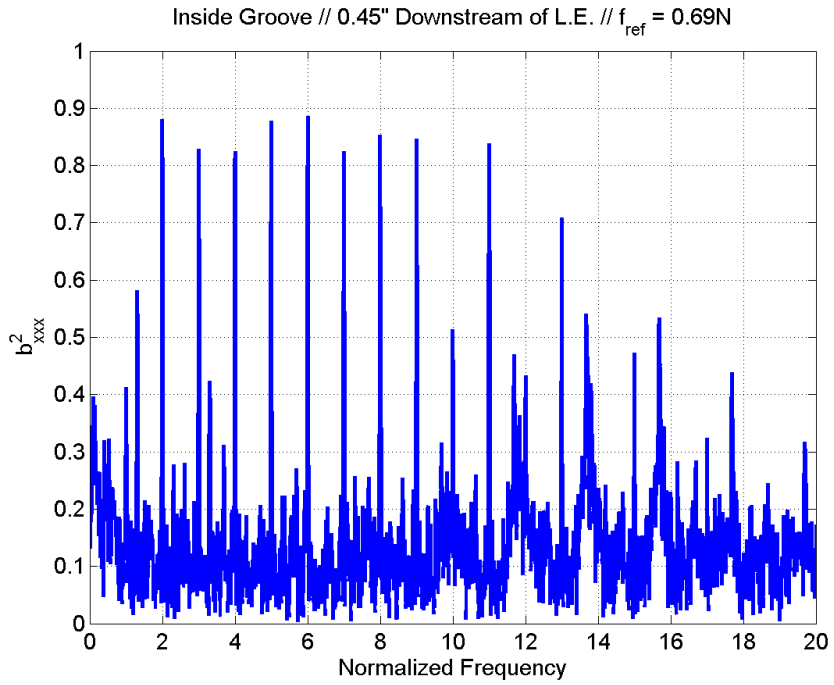

Figure 14: Autobicoherence plot from a measurement in the groove indicating modulation activity between the oscillation at 0.69N and blade passage + harmonics

SUMMARY

Water flow testing of a two blade unshrouded inducer has provided experimental measurements of the hydrodynamic radial load imparted by a cavitation induced oscillation. Furthermore, two shroud treatments were tested to evaluate the effectiveness in reducing or eliminating such a force. Over the hydrodynamic conditions tested, increasing the shroud clearance proved to reduce the radial load by as much as 35% of the baseline value, at the cost of an 18% reduction in head rise. The groove configuration attenuated the radial force by as much as 85% of the baseline value with little to no steady performance loss compared to the other configurations. However, the groove configuration also changed the fluctuating pressure environment around the inducer, resulting in groups of oscillations in the laboratory reference frame. These new oscillations are the result of a new groove induced oscillation that can interact with the blade passage pressure wakes to generate relatively high frequency spatially complex oscillations in the rotating reference frame.

ACKNOWLEDGEMENTS

The authors would like to thank the J2X project office from MSFC for funding the water flow testing. Thanks also go to the Experimental Fluids and Environmental Test Branch at MSFC for the setup and execution of these test series. Yet more thanks go to Tom Zoladz of MSFC and Dr. Sen Meng for their analytical insights and guidance.

References

[1] David M. Cahill, *The AIAA/GTTC Internal Balance Technology Working Group*. First International Symposium on Strain Gage Balances, NASA Langley Research Center, Hampton Virginia, October 1996.

[2] *Allied Aerospace Calibration Report, Balance CDDF2*. 2004.

[3] Shimiya, N., Fujii, A., Horiguchi, H.,Uchiumi, M., Kurokawa, J., and Tsujimoto, Y., *Suppression of Cavitation Instabilities in an Inducer by J-Groove*. ASME Journal of Fluids Engineering, Vol. 130, No. 1 pp. 021302-1-021302-7

[4] Kang, D., Arimoto, Y., Yonezawa, K.,Horiguchi,H., Kawata, Y. Hah,C., and Tsujimoto,Y., *Suppression of Cavitation Instabilities in an Inducer by Circumferential Groove and Explanation of Higher Frequency Components*. International Journal of Fluid Machinery and Systems, Vol. 3, No. 2, April-June 2010.

Fluctuating Pressure Environments and Hydrodynamic Radial Force Mitigation for a Two Blade Unshrouded Inducer

Andrew Mulder and Stephen Skelley

Fluid Dynamics Branch
Propulsion Systems Department
Engineering Directorate
NASA Marshall Space Flight Center
MSFC, AL

Introduction & Objectives

Objectives:

Compare the hydro radial load and fluctuating pressure signatures
Compare hydro radial load across three different shroud configurations

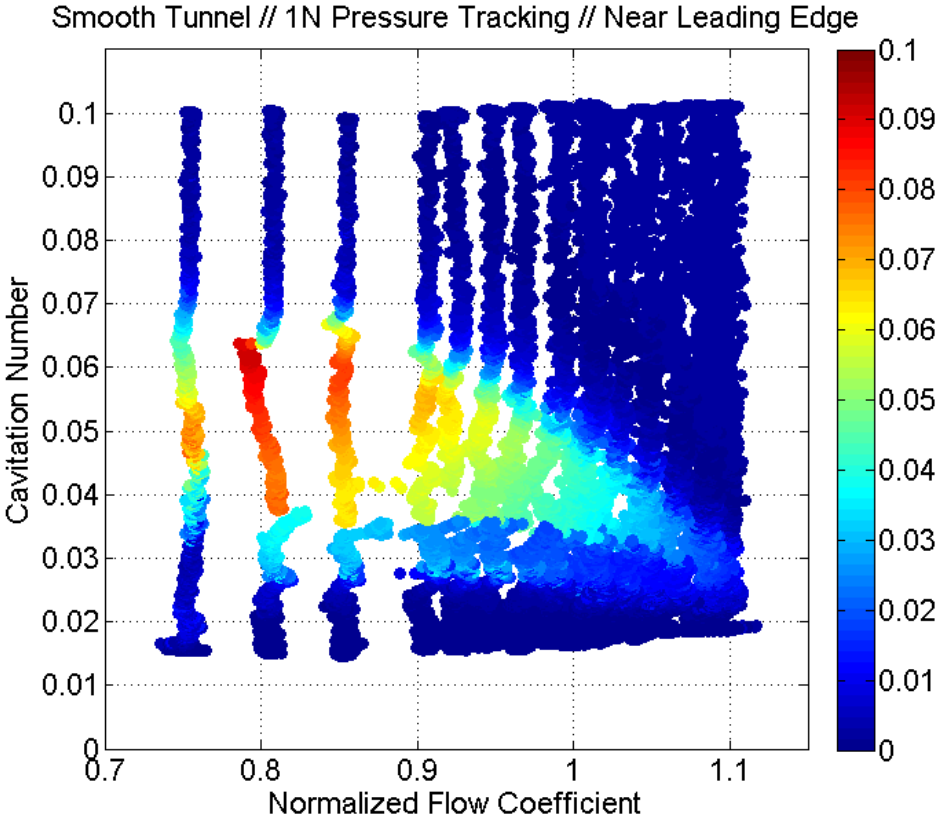

Rotating Balance Installation

Rotating Balance: 3 forces & 3 moments

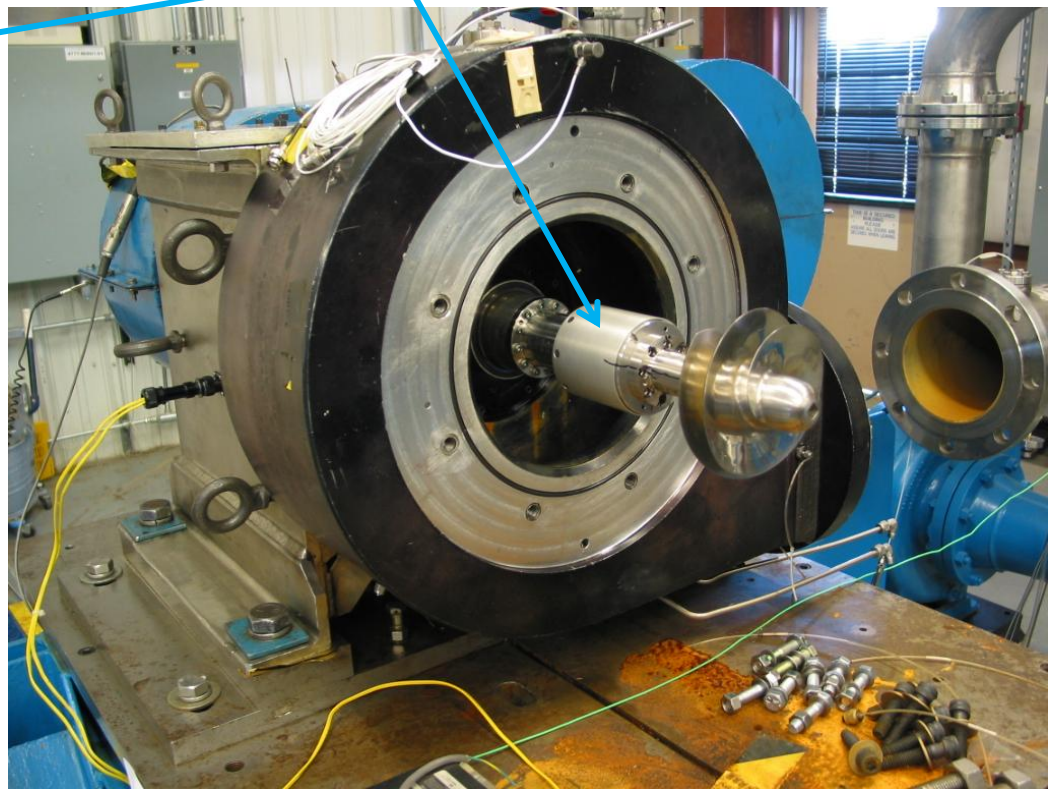

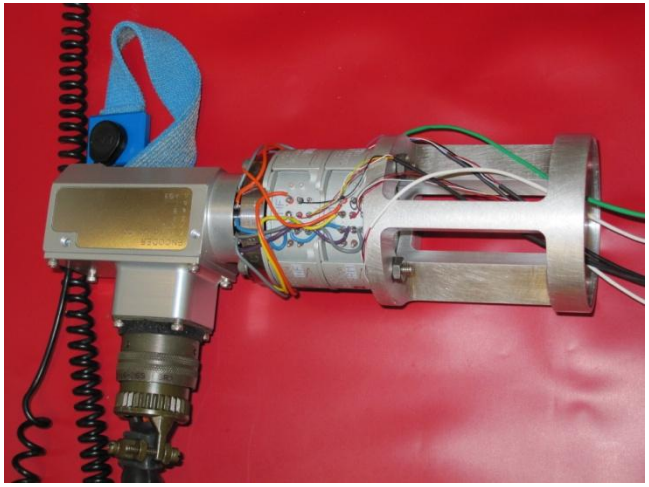

Slip Ring & Rotating Amplifiers

Shroud Configurations

		Configuration		
		1	2	3
A	Inducer Outer Diameter (inch)	---------- 5.075 ----------		
B	Inducer Radial Clearance (inch)	0.015	0.027	0.014
C	Groove Outer Diameter (inch)	n/a	n/a	5.775
D	Groove Width (inch)	n/a	n/a	0.661
	Clearance (% Blade Height)	0.86%	1.55%	0.81%
	Groove CL to LE Tip (inch)	n/a	n/a	0.211

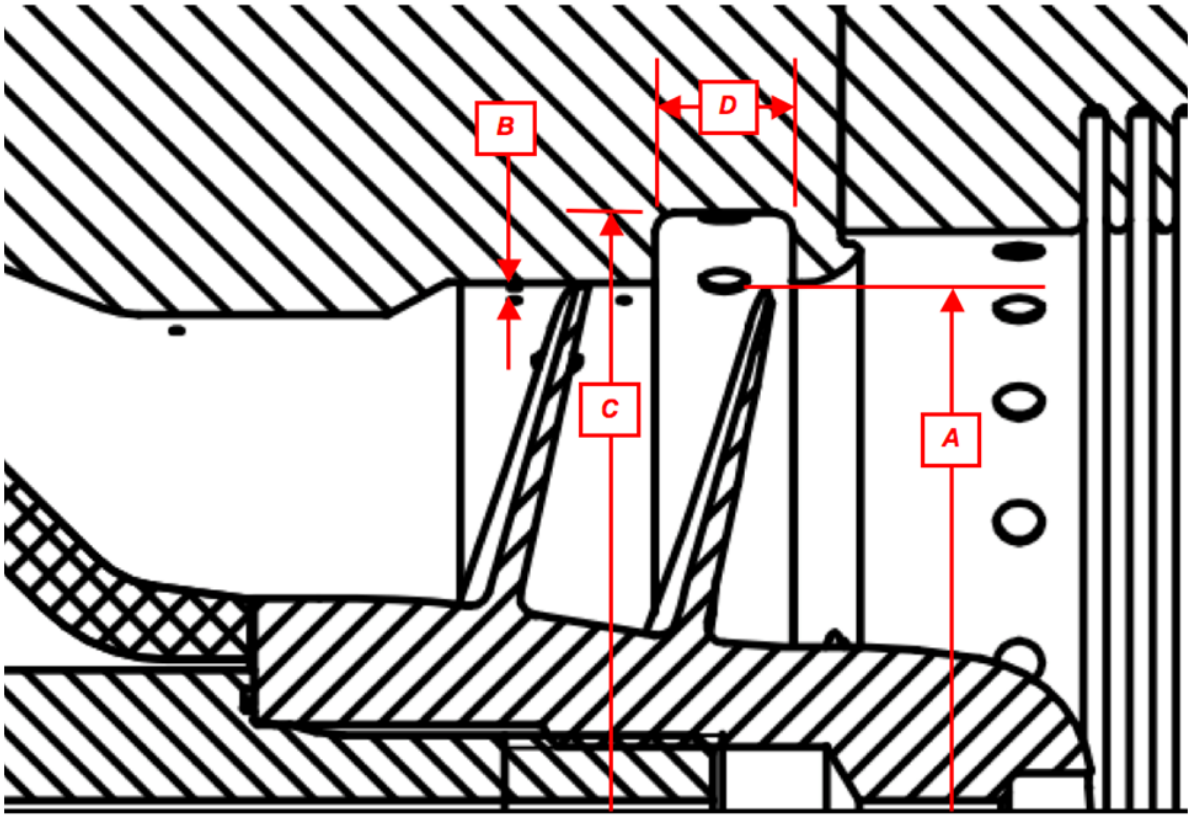

Force Measurement Results

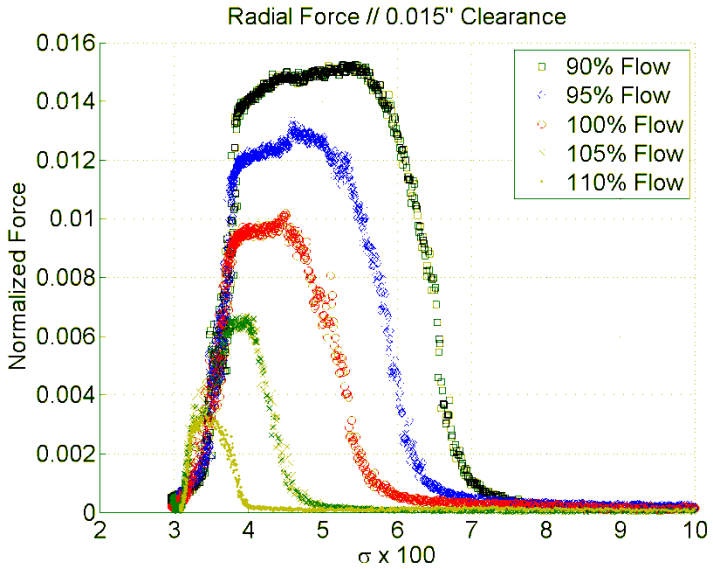

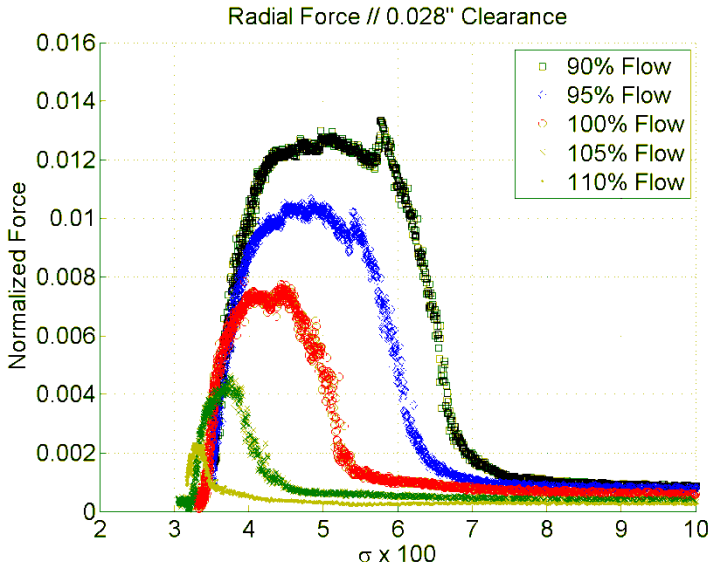

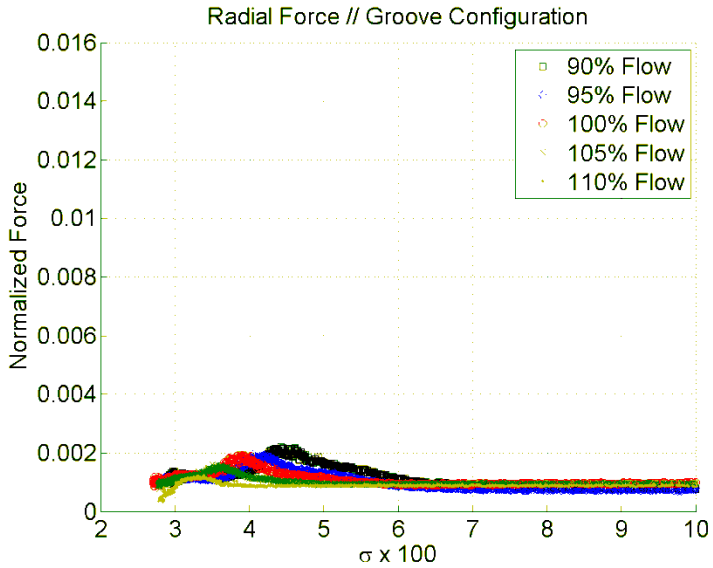

Across all tested flow coefficients, nearly doubling the radial clearance resulted in a modest decrease in hydro radial load

The introduction of the groove significantly reduced the hydro radial load

Force / Pressure Comparison

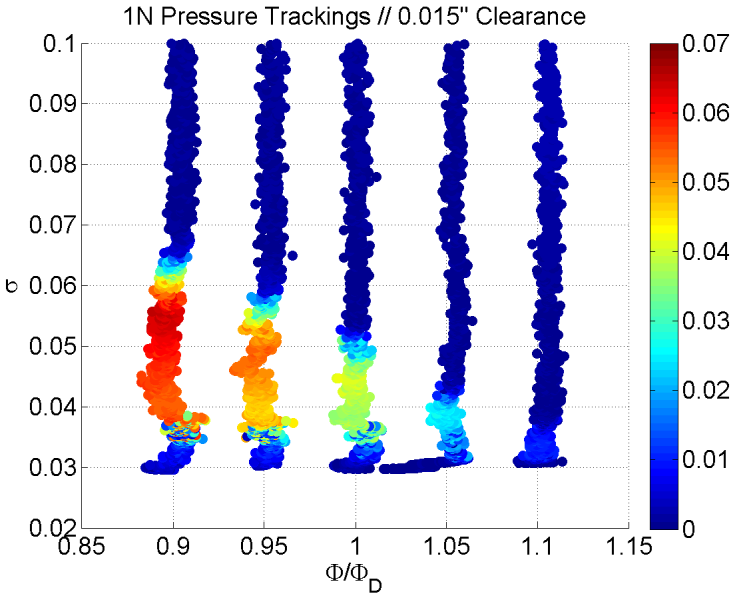

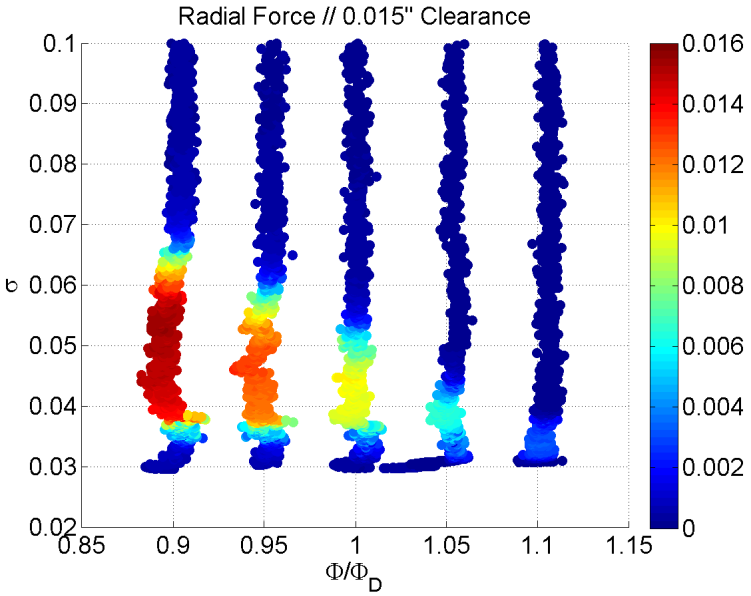

Synchronous pressure and force amplitude appear to share incidence and desinence conditions

The pressure/force relationship is linear

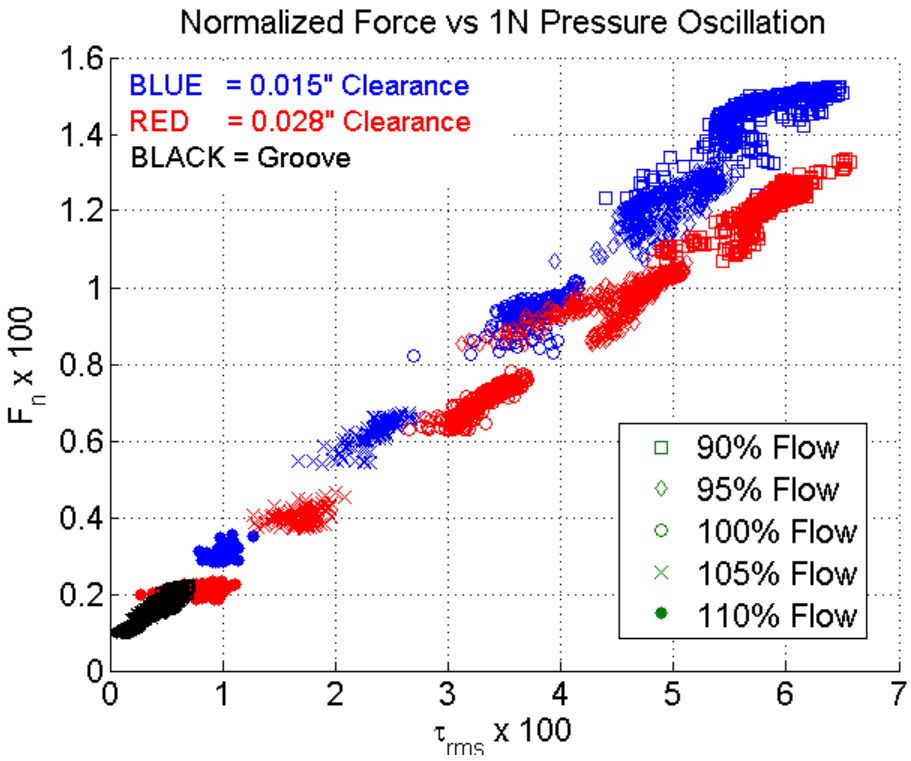

Fluctuating Pressure Environment

Smooth Tunnel

Blade passage / 1N / Surge
1N & 2N harmonics

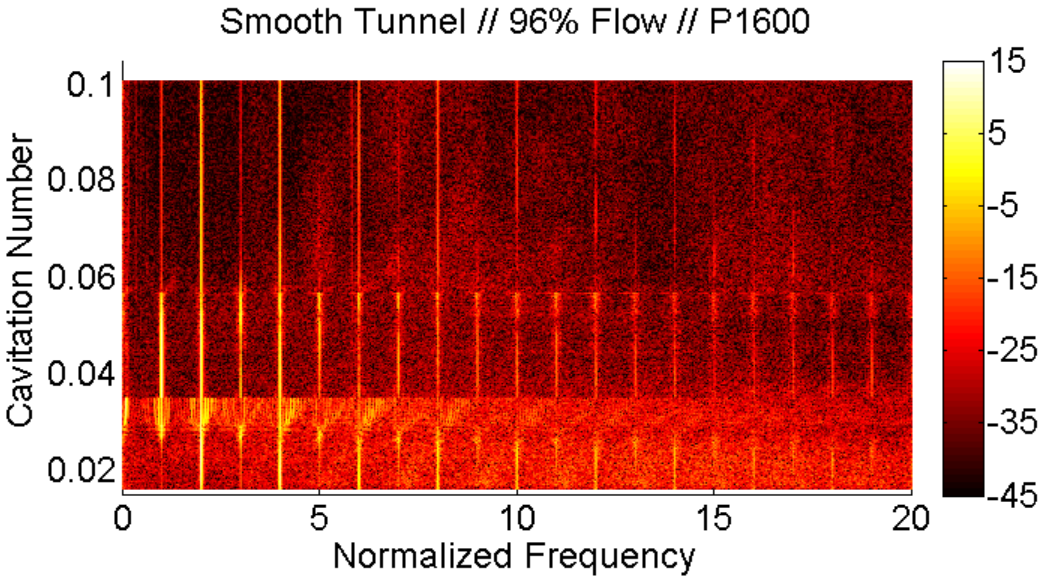

Grooved Tunnel

Blade passage always high
1N & Surge reduced or gone
Multiple oscillations at off sync multiples

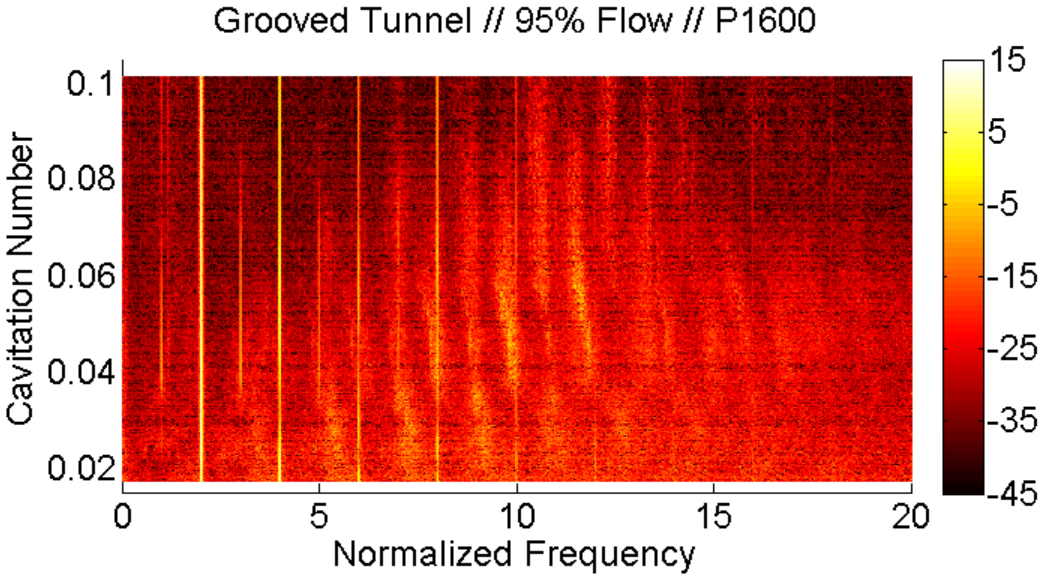

Fluctuating Pressure Environment

These oscillations vary in spatial complexity and frequency depending on operating conditions

110% Flow

75% Flow

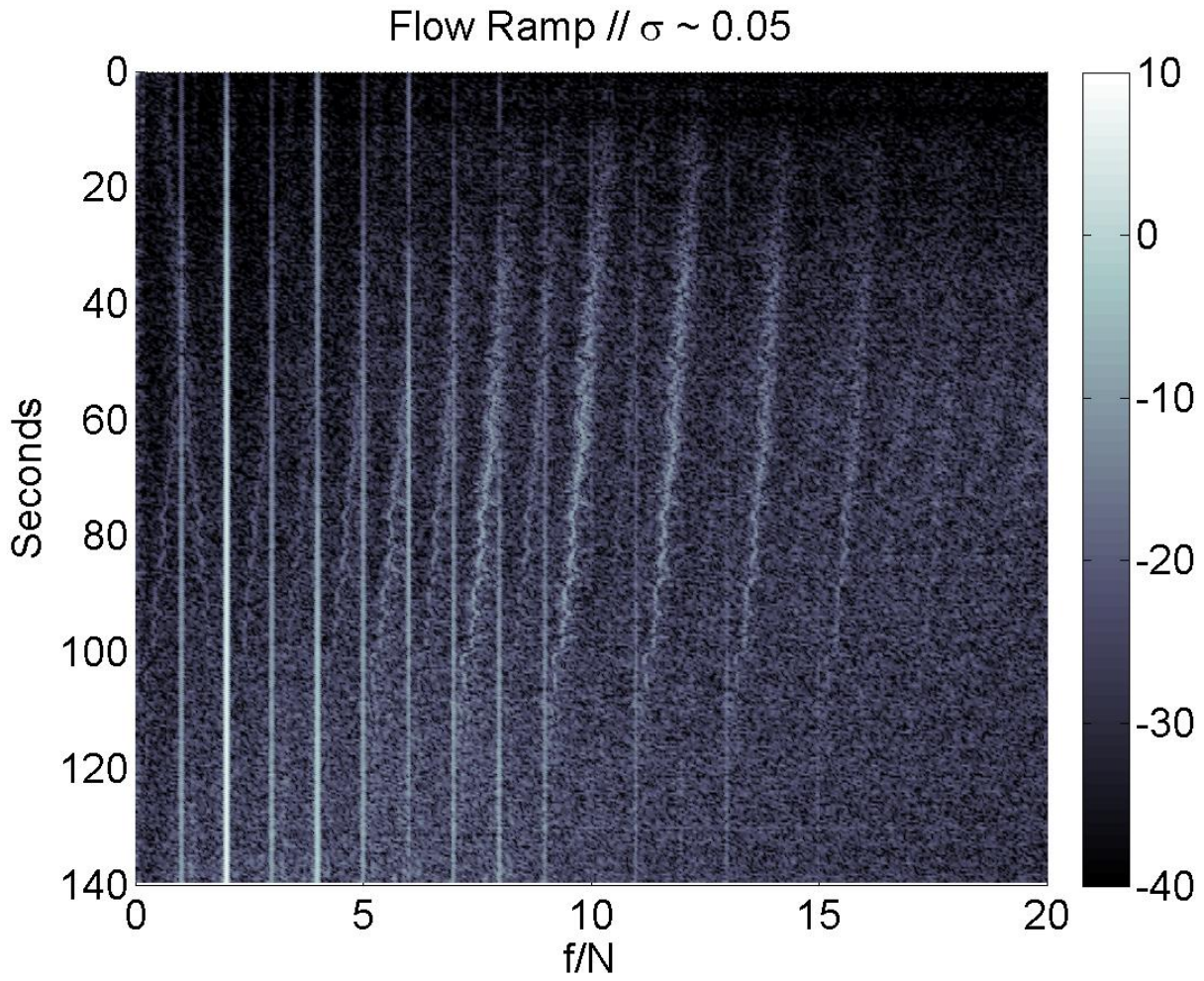

Fluctuating Pressure Environment

These groups of oscillations map to single frequencies in the rotating frame

$f_r = f_{lab} + kf_n$

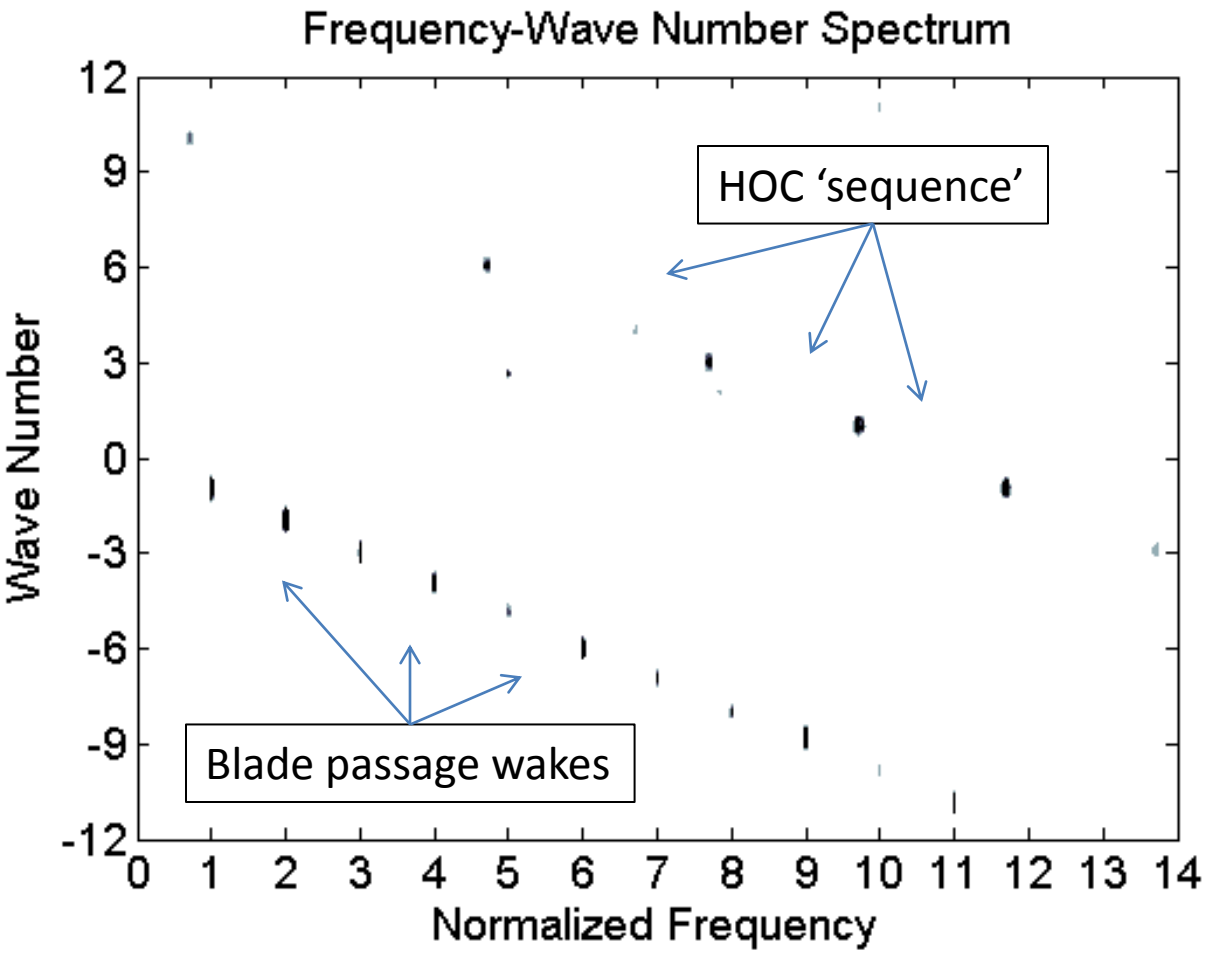

$\sigma \sim 0.05$
95% flow
Inside Groove

Fluctuating Pressure Environment

These oscillations modulate with synchronous + blade wakes + harmonics
Each oscillation has high auto-bicoherence with synchronous multiples

Example: 0.69N // ~92% flow // σ ~ 0.05

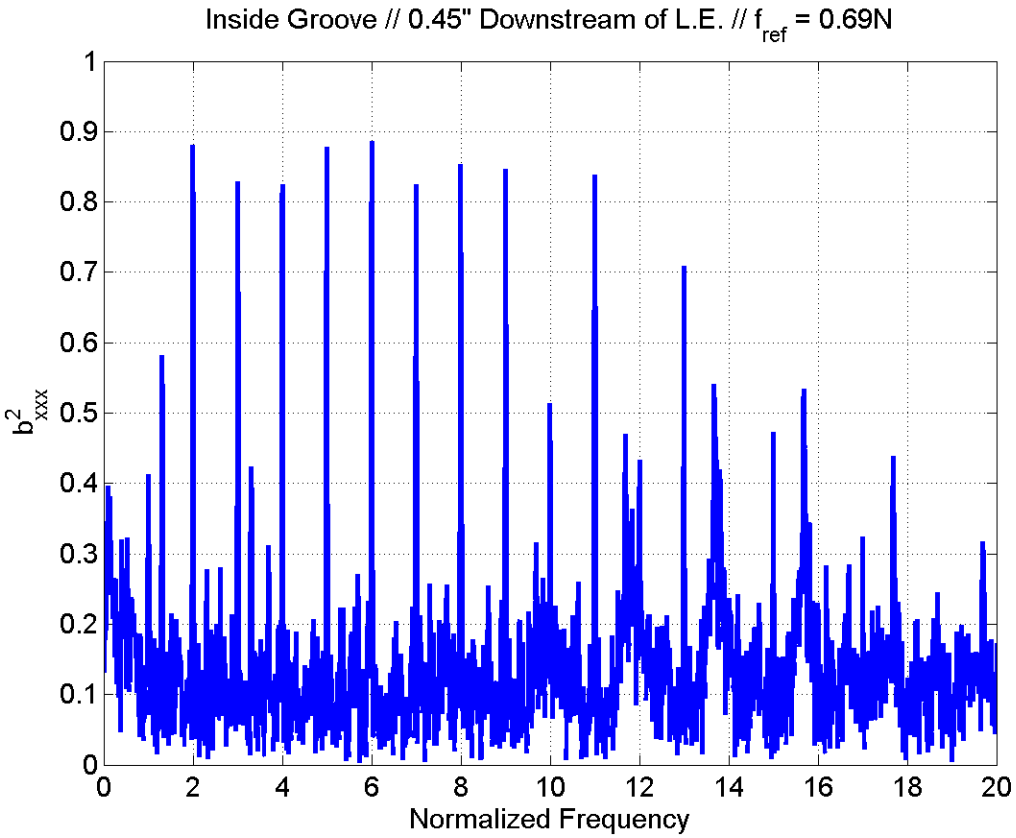

Summary

Initial water flow testing of a 2 blade unshrouded inducer indicated a potential hydrodynamic radial load due to 1N cavitation

After measuring the radial force in a smooth tunnel, 2 shroud configurations were tested for load mitigation

Uniformly increasing the blade clearance resulted in some load reduction

A circumferential groove resulted in large load reduction by virtually eliminating the 1N cavitation instability

The groove also introduced relatively high frequency spatially complex oscillations to the pressure environment

The oscillations are likely due to the interaction of swirling back flow with the blade passage process and the incident bulk flow